abundance (*3*). We normalized the AD values to "frequency" values by referring the AD values on each chip to a calibration curve constructed from the AD values for the 11 control transcripts with known abundances that were spiked into each hybridization (*9*). This "frequency normalization" allowed comparison of transcript measurements across multiple array experiments. Frequency values for each gene were expressed in number concentrations (transcripts per million, or ppm), under the assumptions described (*9*).
13. P. Tamayo *et al.*, *Proc. Natl. Acad. Sci. U.S.A.* **96**, 2907 (1999).
14. Supplemental information is available at www.sciencemag.org/feature/data/1053496.shl.
15. I. L. Johnstone, J. D. Barry, *EMBO J.* **15**, 3633 (1996).
16. M. C. Costanzo *et al.*, *Nucleic Acids Res.* **28**, 73 (2000). (The Proteome WormPD database is available at http://www.proteome.com/databases/index.html).
17. C. E. Rocheleau *et al.*, *Cell* **90**, 707 (1997).
18. P. W. Carter, J. M. Roos, K. J. Kemphues, *Mol. Gen. Genet.* **221**, 72 (1990).
19. Additional details are available as supplemental information (*14*).
20. J. H. Xin, B. P. Brandhorst, R. J. Britten, E. H. Davidson, *Dev. Biol.* **89**, 527 (1982).
21. S. A. Chervitz *et al.*, *Science* **282**, 2022 (1998).
22. G. M. Rubin *et al.*, *Science* **287**, 2204 (2000).
23. To classify worm genes, we used the sequence comparison results of Rubin *et al.* (*22*). In the period between the date of our chip design (early 1999) and the date of this more recent sequence comparison (early 2000), some of the worm ORFs that had been included in the chip designs had been deleted or altered by worm sequence curators (for details on the curation of the Wormpep database, see http://www.sanger.ac.uk/Projects/C_elegans/wormpep/). To reconcile worm ORFs in the sequence comparison with worm ORFs on the arrays, we limited our analysis to worm ORFs on the arrays that were unchanged between the two data sets, using curation lists maintained at the Sanger Centre (the Wormpep.history file). Thus, we identified on the arrays 2905 worm genes shared between yeast, worm, and fly (core genes); 3150 worm genes shared between worm and fly, but not yeast (animal genes); and 8741 worm genes that were unique to the worm (worm genes). Shared worm genes were defined as those that had significant homology to one or more genes in yeast or fly (BLASTP expectation values $E < 1 \times 10^{-10}$, as described by Rubin *et al.*) Discrepancies between these numbers of ORFs and comparable counts in Rubin *et al.* are accounted for by the facts (i) that 2% of worm ORFs were not monitored directly by the arrays and (ii) that, to be conservative, we excluded from consideration ORFs that had either been deleted or altered in the Wormpep database in the interval between the chip design and the sequence comparison of Rubin *et al.*
24. We thank M. Whitley for advice on array experiments; K. Griffiths for array bioinformatics support; E. Wilson, A. Velasco, and H. Horton for technical assistance; J. Freeman for bioinformatics support during the chip design process; G. Sherlock for sharing yeast and worm sequence comparison data; M. Yandell for sharing yeast, fly, and worm sequence comparison data; and D. Mootz for providing purified oocytes.

26 June 2000; accepted 29 September 2000

Song Replay During Sleep and Computational Rules for Sensorimotor Vocal Learning

Amish S. Dave and Daniel Margoliash*

Songbirds learn a correspondence between vocal-motor output and auditory feedback during development. For neurons in a motor cortex analog of adult zebra finches, we show that the timing and structure of activity elicited by the playback of song during sleep matches activity during daytime singing. The motor activity leads syllables, and the matching sensory response depends on a sequence of typically up to three of the preceding syllables. Thus, sensorimotor correspondence is reflected in temporally precise activity patterns of single neurons that use long sensory memories to predict syllable sequences. Additionally, "spontaneous" activity of these neurons during sleep matches their sensorimotor activity, a form of song "replay." These data suggest a model whereby sensorimotor correspondences are stored during singing but do not modify behavior, and off-line comparison (e.g., during sleep) of rehearsed motor output and predicted sensory feedback is used to adaptively shape motor output.

In reinforcement learning, systems learn through interaction with the environment by trying to optimize some measure of performance. Biological systems may experience a substantial delay between premotor activity and assessment of performance through sensory feedback (*1*). This delay poses the problem of how to reward or punish a premotor circuit when that circuit is participating in a different task by the time the reward or punishment is computed. Reinforcement learning is further complicated in systems such as vocal learning, where the mapping of sensory feedback (fundamentally represented as frequency versus time) onto motor output (muscle dynamics) is of high dimensionality (a many-to-many dynamic mapping). Methods developed in the field of machine learning solve the problem of reinforcement learning with delayed reward (*2*), and a variety of biological solutions have been proposed to the problem of learning sequences of actions (*3*). Here, we report on neuronal data that represent a solution to the problem of sensorimotor mapping in the bird vocal-motor ("song") system. The physiological properties observed during sleep also suggest an algorithmic implementation for reinforcement learning of song.

Zebra finch songs are organized hierarchically, with one or more notes composing a syllable, and sequences of syllables forming a motif, which are repeated to form song. We investigated neurons in the forebrain nucleus robustus archistriatalis (RA), whose descending projections represent the output of the forebrain song system. During singing, RA neurons exhibit short bursts of activity, whose identity varies with the note that immediately follows the burst (*4*). In awake birds, outside the context of vocalizations, RA neurons are regularly firing. RA neurons also prominently burst "spontaneously" and respond to sounds, but only during sleep (*5*). With the goal of comparing motor, auditory, and ongoing bursting activity, we recorded single neurons in the RA of singing male zebra finches, permitted the animals to fall asleep by turning off the lights, and then tested the same neurons' sensory and ongoing discharge properties (*6, 7*).

The spiking patterns of RA neurons in singing birds consisted of phasic patterns of premotor excitation superimposed over a background of profound inhibition (*4*) (Fig. 1, B and C). This premotor activity was virtually invariant for multiple occurrences of the same sound. After the lights were turned off, RA auditory responses were initially weak but gained strength with time, reflecting the gradual transition into sleep (*5*). Responses to playback of the bird's own song (BOS) also consisted of phasic patterns of excitation separated by inhibition that were similar for multiple occurrences of the same sound, differing mainly in the strength of response rather than pattern (*8*).

The timing of auditory responses to the BOS was very well aligned to the timing of premotor activity (Fig. 1F). The only exceptions were instances of silence following the end of a motif or the end of song, where the auditory response could include an additional burst that corresponded with the syllable that would have followed if the song had continued without pause. To compare motor and auditory activity, we analyzed the singing-related activity surrounding each syllable of song (*4*, *9*). The spike patterns from the response to the BOS playback were then compared with the spike patterns from premotor activity derived from

Department of Organismal Biology and Anatomy, University of Chicago, 1027 East 57 Street, Chicago, IL 60637, USA.

*To whom correspondence should be addressed. E-mail: dan@bigbird.uchicago.edu

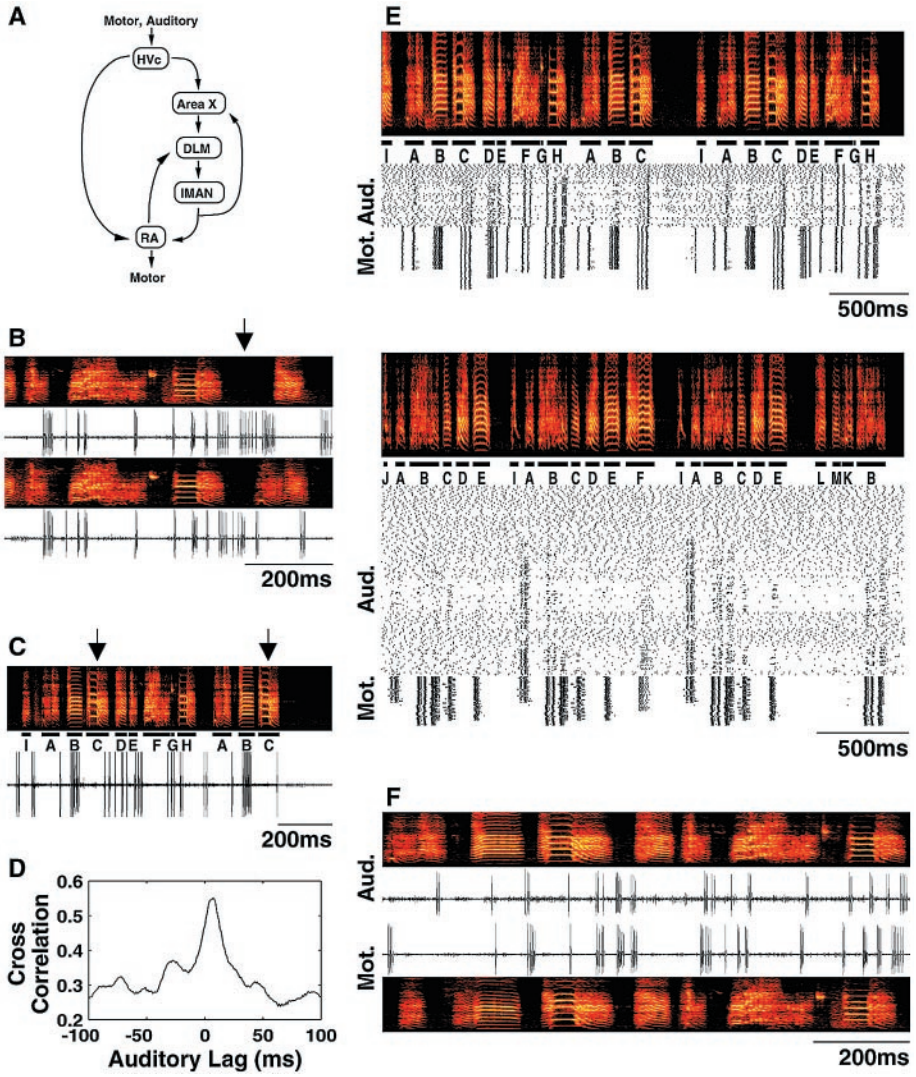

Fig. 1. (**A**) Schematic of the song system. Auditory and premotor activity converge onto the HVc. The HVc projects directly to the RA, which projects to brainstem motor centers. The HVc also projects to area X, which projects to the DLM. The DLM projects to the lMAN, which projects to the RA. Feedback loops arise from the RA and lMAN. (**B** and **C**) Activity of RA single neurons during singing is premotor (i.e., neuronal activity leads syllables). Spectrographs of the sound that the bird produced are shown in a color scale (frequency, 0 to 10 kHz, is on the ordinate; time is on the abscissa). Corresponding raw traces of the neural activity (amplitude versus time) are shown below the spectrographs. Data from one neuron for two similar examples of singing are shown in (B). The neuron's activity patterns are the same for the two examples of singing, except where the vocalizations differ, and the difference in neuronal discharge (at arrow) precedes the difference in the vocalizations. Both sequences of vocalizations occurred frequently; the neuronal pattern associated with each sequence was stereotyped. In (C) [different neuron, same bird as in (B)], the bird produced syllable "C" (marked by arrows) twice (each syllable is identified by a letter), with the song ending prematurely after the second occurrence. The neuronal discharge following the second C was affected. Activity during calling (not shown) also clearly demonstrates that RA activity leads vocalizations [see also (*4*)]. (**D**) Cross-correlation of auditory and motor activity for the first neuron shown in (**E**) (positive time shifts imply that auditory response lags premotor activity). (E) Examples of the match between auditory and motor activity from one neuron in each of two birds. The spectrographs show the BOS used as stimuli during playback experiments, and each syllable is identified by a letter. The rasters marked "Aud." represent the neuron's auditory response during playback while the birds were asleep. The rasters marked "Mot." were constructed from neuronal activity of the same neurons during singing (*4*). The correspondence between the two patterns of activity is visually striking. In contrast to singing, however, during song playback, neurons exhibited ongoing discharge, not inhibition, for some syllables. (**F**) Example of raw traces showing the match between activity during playback and singing [same neuron as in (B)].

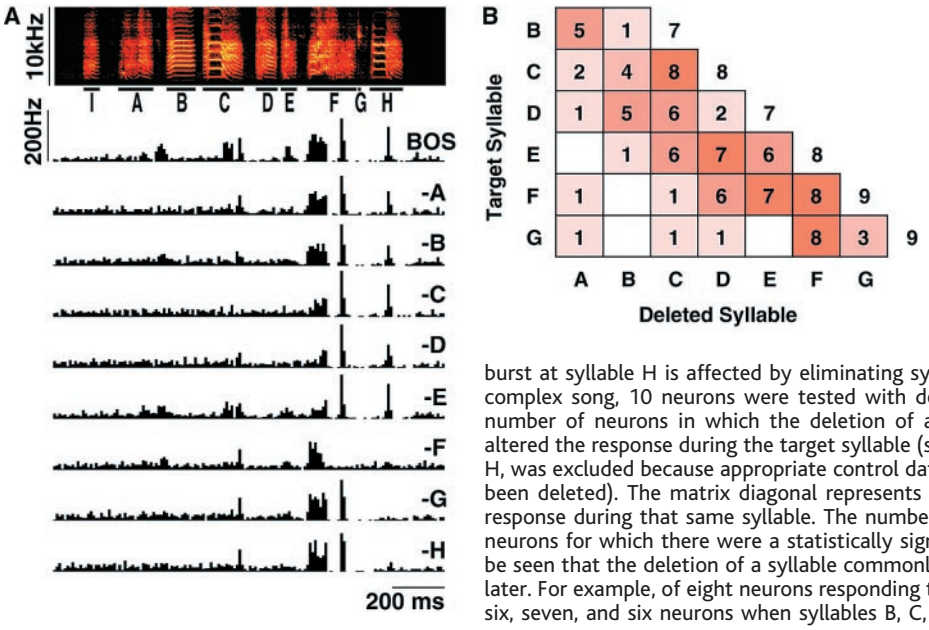

Fig. 2. Deletion experiments. (**A**) The bird was presented songs during sleep. Below the spectrograph of the last motif of the bird's song are nine histograms of the response of one neuron, representing 30 repetitions each of nine different stimuli. The BOS histogram is the response to the unaltered motif. For each of the eight other stimuli, one of the syllables from A to H was replaced with background noise. For syllable F, for example, the neuron responded with two bursts, with both bursts occurring during syllable F. The first burst (but not the second) is statistically significantly reduced (*8*) by the elimination of syllables C, D, E, or F. The second burst is affected by the elimination of syllable F. The burst at syllable H is affected by eliminating syllables F, G, and H. (**B**) In one bird with the most complex song, 10 neurons were tested with deletion stimuli. Each cell of the matrix gives the number of neurons in which the deletion of a syllable (specified by the column) significantly altered the response during the target syllable (specified by the row). The last syllable of the song, H, was excluded because appropriate control data were unavailable (an earlier syllable had always been deleted). The matrix diagonal represents the effect of deleting a syllable on the neuronal response during that same syllable. The numbers to the right of the diagonal are the number of neurons for which there were a statistically significant response during the target syllable. It can be seen that the deletion of a syllable commonly affected the neuronal response several syllables later. For example, of eight neurons responding to syllable E, the response was suppressed for one, six, seven, and six neurons when syllables B, C, D, and E, respectively, were deleted.

the corresponding syllables, showing that the timing of excitation and inhibition during auditory stimulation was well aligned to such timing during singing (Fig. 1, D and E). A cross-correlation procedure revealed a strong, significant ($P < 0.02$) correlation (*10*) between premotor and sensory spike patterns in all 17 neurons (from three birds) (mean normalized peak correlation = 0.49 ± 0.13 SD). Thus, sensorimotor transformations in the song system result in a correspondence between temporally precise sensory and motor activity observed at the level of individual cells.

The auditory activity was only slightly delayed in relation to motor activity (by 8 ± 2 ms; range, 4 to 13 ms). Because premotor activity in RA can lead the onset of syllables by up to ~40 ms (*4*), this was surprising and suggested that the sensory patterns representing subsequent syllables were generated by responses to previous syllables. To characterize the extent of temporal integration in the auditory responses, we presented stimuli in which a syllable chosen at random from the final motif of the BOS was substituted by a background of equal duration, and we assessed the effect on the neuronal activity during the same or subsequent syllables (*11*). The deletion of a syllable substantially reduced the neuronal activity occurring one to three syllables later (Fig. 2A), up to ~250 ms (*8*). This property was ubiquitous for all RA neurons that were auditory (14 neurons from three birds) (*12*) (Fig. 2B). These response properties are suggestive of temporal combination sensitivity, in which a sensory neuron's response is nonlinearly dependent on the temporal sequence of preceding syllables. Such responses have also been described for neurons in the nucleus HVc, which projects to the RA (*13*). Thus, in the RA as well as in the HVc (*4, 13*), the integration time of individual neurons appears to be considerably greater when in the sensory (auditory) state than during singing. Given the alignment of auditory and motor activity in the RA, one way of interpreting these results is that auditory responses to song syllables represent a prediction of subsequent premotor activity.

We also searched for similarities between ongoing bursting activity during sleep (*5*) and the sensorimotor patterns of RA neurons. For each cell, a visual inspection of samples of activity from long stretches (15 to 60 min) of undisturbed sleep identified repeated examples of one or more complex burst patterns, suggestive of the patterns that we had observed in the cell's premotor activity. To quantify this match, we developed a procedure to automate burst detection (*14*), considering only bursts of eight spikes or more to ease the computational burden and to allow for statistical analysis. By this procedure, 7.1 ± 5.3% of all spikes (14 neurons from three birds) occurred in bursts, an average of 175.4 ± 144.6 (range, 38 to 581) bursts per cell. For each cell, a measure of similarity between each burst and the single longest bout of the cell's premotor activity (4 to 8 s, consisting of several motifs or songs) was computed and tested for significance (*15, 16*). The results showed that 15.3 ± 6.5% of bursts (range, 2.6 to 26.8%) significantly matched premotor activity. Only the cell with 2.6% matching bursts failed to exceed the 5% level expected by chance (*16*). Examples of matches between longer sequences of complex ongoing bursts and premotor activity were particularly compelling (Fig. 3A). In an exceptional case when two RA neurons were recorded simultaneously from different electrodes during sleep, both neurons commonly exhibited simultaneous bursting, with the different burst patterns for each neuron corresponding to the same sequences of syllables (Fig. 3B). This suggests that populations of RA neurons burst in a coordinated fashion during sleep. Bursts (and matching bursts) preferentially occurred during periods when the rate of ongoing discharge was lower and more variable (Fig. 4). Such modulation may

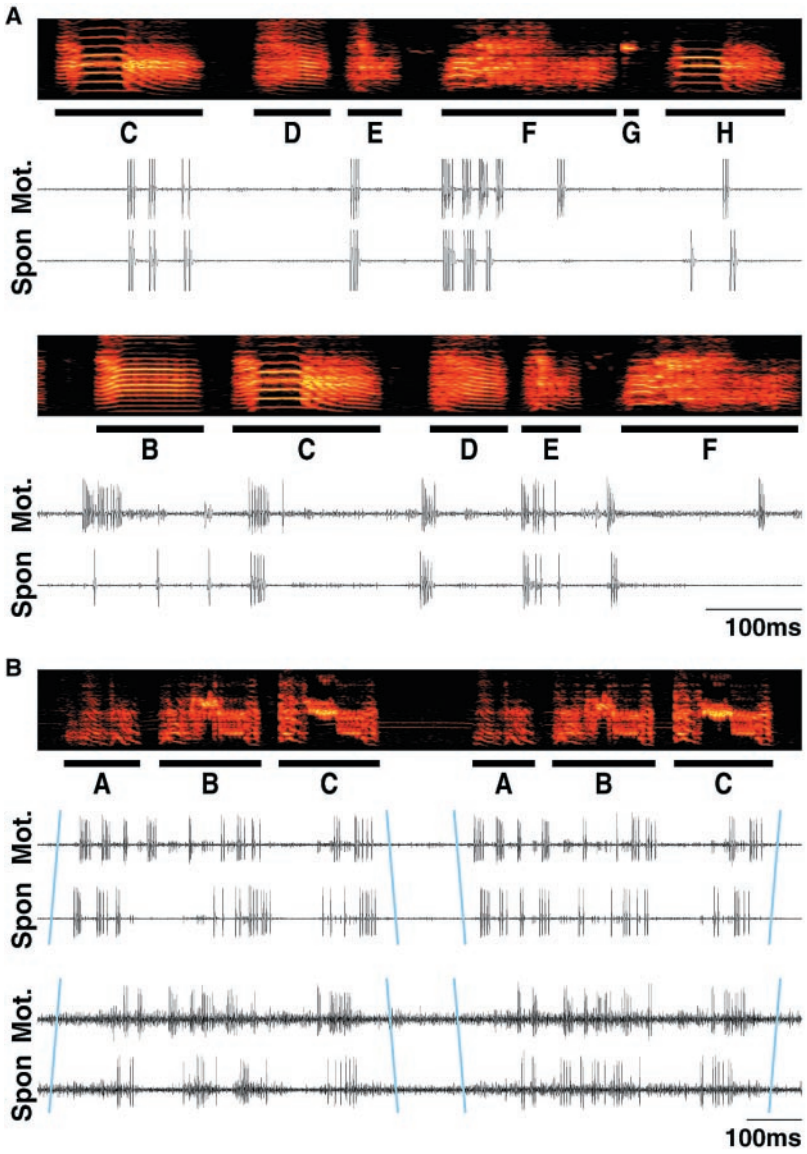

Fig. 3. Neuronal replay during undisturbed sleep. (**A**) Raw traces of neuronal activity (900 ms) during sleep ("Spon") in two different neurons for one bird. For each sample, a representative corresponding sample of premotor activity ("Mot.") and a color spectrograph of the song that the bird sang are shown. (**B**) Raw traces (1400 ms) of simultaneous recordings from two neurons (~400 μm apart) in another bird. (The second neuron's activity is visible in the background of the first neuron's signal, an artifact of the pairing of signals used to achieve differential recordings resistant to movement-induced artifacts.) Both neurons simultaneously burst during sleep, with complex burst structures that match premotor activity. Apparent temporal expansion (first motif: A, B, and C) and compression (second motif: A, B, and C) is highlighted by the blue lines. This phenomenon has also been reported in population activity of hippocampal neurons (*23*).

correspond to specific phases of the sleep cycle.

In the sensorimotor phase of vocal learning, the mapping between auditory feedback and vocal output is the fundamental computational problem to be solved (*17*). A solution to this problem is reflected in the sensorimotor activity patterns of RA neurons. Precision of spike timing has been observed in a number of systems and provides evidence for temporally based neural codes in sensory processing, although only in a few cases has the behavioral relevance been directly demonstrated (*18*). The observed correspondence between auditory activity and vocal output demonstrates that, in the RA, sensorimotor mapping is based on a temporal code. This correspondence is likely to arise from auditory input recruiting similar components of the RA pattern-generating circuits as those recruited during singing. In the hierarchical organization of the song system (*4, 19*), the sensorimotor correspondence may first emerge at the single-cell level within the RA. The data suggest that, during vocal development, the song system learns to generate premotor commands by association with a prediction of future commands based on the timing of auditory feedback from preceding syllables. This can be interpreted as learning the match between the auditory response to a sequence of syllables with the premotor pattern for a subsequent syllable or as learning the match between the prediction of a sensory representation of a syllable with the premotor representation of the same syllable.

In the birdsong system, RA receives input from the HVc and from an anterior forebrain pathway (AFP) (Fig. 1A). Sensorimotor song learning could result in part from "online" mechanisms, whereby during singing, HVc activity in response to auditory feedback from sequences of syllables is delayed through the AFP to produce a prediction of activity in the RA of a subsequent syllable. The data collected during sleep, however, also suggest "off-line" models for learning that address the problems of feedback delay and sequence generation. Such models share some similarities with temporal-difference models of reinforcement learning and sequence generation that are prominent in mammalian work on basal ganglia and the cerebellum, in that they reward or modify the system on the basis of its overall performance, not on the basis of the performance of individual components or movements (*3*). The AFP has been likened to a mammalian corticobasal ganglia-thalamocortical loop (*20, 21*).

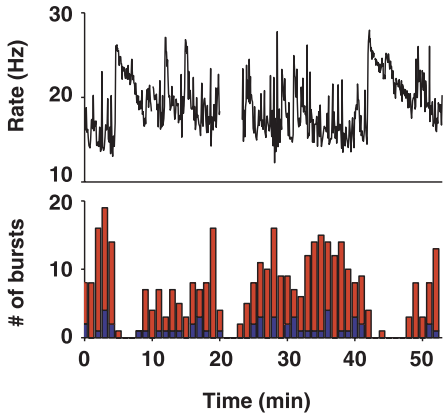

Fig. 4. (**Top**) The firing rate during recordings of RA ongoing activity over almost 1 hour of sleep, estimated from a 100-point moving average of the interspike intervals (there was a gap in the data collection of ~3.25 min). (**Bottom**) A histogram (30-s bins) of the number of bursts identified by a burst-finding procedure. The number of bursts that significantly matched the premotor activity is shown in blue.

In the vocal learning model motivated by the present data, signals that arise in the RA during singing train the AFP to generate a prediction of auditory feedback; during sleep rehearsal, the AFP's predicted feedback provides reinforcement to RA neurons. During singing, sensorimotor efference copy signals (premotor output and expected auditory feedback) traverse the AFP, and via the lateral subdivision of the magnocellular nucleus of the anterior neostriatum (lMAN) projection onto area X, are compared with real auditory feedback arriving in area X from the HVc (Fig. 1A). Efference copy is brought into temporal register with auditory feedback using the long (~50 ms) synaptic delays observed in the medial subdivision of the dorsolateral nucleus of the thalamus (DLM) (*21*). This stimulates area X neurons that are sensitive to temporally coincident input. The output of the lMAN onto the RA has a reduced effect because the lMAN is not in temporal register with driving input from the HVc. During sleep, replay of song premotor patterns via ongoing bursting generates coherent activity throughout the song system that is similar to singing in the absence of actual sound production and perception. The output of the lMAN represents a prediction of the real auditory feedback that would have resulted from the burst-generated motor command, is in near coincidence with HVc bursts driving the RA, and is used to modify RA neurons that are sensitive to temporally coincident input.

The proposed algorithm for birdsong learning depends on circadian modulation of neuronal activity patterns (*22*). Our observation of neuronal replay of sensorimotor patterns during sleep is consistent with data from hippocampal studies suggesting that sleep is important for the consolidation of neuronal temporal codes for spatial memory (*23, 24*). The fundamental prediction of our model is that birdsong learning depends on sleep or other off-line computations.

References and Notes

1. In songbirds, there is a minimum delay of ~70 ms or longer between the production of a burst of neuronal activity contributing to song generation and the reception of processed auditory input from the resulting vocalization. In zebra finches, syllables are typically 50 to 200 ms in duration and may comprise one or several notes. The minimal delay is the sum of premotor lead (~50 ms) and sensory lag. Sensory lag is the sum of the minimal latency for response (~20 ms) and the sensory integration time, which, for song system neurons, can be tens to hundreds of milliseconds.
2. R. S. Sutton, A. G. Barto, *Reinforcement Learning: An Introduction* (MIT Press, London, 1998).
3. R. E. Suri, W. Schultz, *Exp. Brain Res.* **121**, 350 (1998); D. G. Beiser, J. C. Houk, *J. Neurophysiol.* **79**, 3168 (1998); G. S. Berns, T. J. Sejnowski, *J. Cogn. Neurosci.* **10**, 108 (1998); J. Brown, D. Bullock, S. Grossberg, *J. Neurosci.* **19**, 10502 (1999).
4. A. C. Yu, D. Margoliash, *Science* **273**, 1871 (1996).
5. A. S. Dave, A. C. Yu, D. Margoliash, *Science* **282**, 2250 (1998)
6. All neuronal data reported in this report are from single units. Eighteen neurons (10, 5, and 3) from three birds contributed to the data reported herein. Two additional neurons from a fourth bird exhibited a match between auditory responses and ongoing bursts. These data were the genesis for this study but did not include premotor data.
7. The chronic recording procedures and conduct of the experiments are described in detail on *Science* Online (*24*).
8. Additional procedures and data regarding the auditory responses of the neurons are described on *Science* Online (*24*).
9. The pattern of RA neuronal activity depends on notes, which are constituents of syllables. By definition, the same pattern of notes is repeated for a given syllable type. We analyzed RA activity at the syllable level to ease the analysis and to minimize the number of deletion stimuli required in subsequent experiments. Following established procedures, we identified each syllable that the bird sang, and the times of onset and offset were manually determined from spectrographs and oscillographs of the acoustic signal. The spectrographs of all exemplars for each syllable type were cross-correlated to establish optimal time shifts; these were then applied to the corresponding spike bursts. The aligned time-shifted spikes were the basis for further analysis.
10. Peak cross-correlation values were tested for significance by using a bootstrap procedure, described in detail on *Science* Online (*24*).
11. Multiple stimuli were derived from the BOS, one for each syllable deleted from the last complete motif of the BOS; these were presented in one block during the night while the bird was asleep. Deleted syllables were replaced with samples from silent intervals between motifs or syllables. Spike rates were computed over the duration of each syllable. For each syllable from the second to the penultimate, we compared the spike rates over the interval of the target syllable when a previous syllable or the target syllable itself was deleted (experimental data) against the spike rates for the target syllable when only a subsequent syllable was deleted (control data), using a Mann-Whitney *U* test at the 95% confidence level. The last syllable in the song was excluded because, by definition, control data were not available. (The response to the BOS, presented at the beginning of the night's recordings as the bird transitioned into sleep, showed fluctuations in the strength of response but not in the timing of spikes. Thus, it was appropriate for correlation testing of sensorimotor comparisons but not for a comparison with spike counts of deleted syllable stimuli.)
12. The three birds presented with deletion stimuli had songs with eight, five, and three syllables per motif. All 10 neurons tested in the eight-syllable bird (Fig. 2B) and all 3 neurons tested in the three-syllable bird showed a loss of excitatory response when the target or a previous syllable was deleted. One of two neurons tested in the five-syllable bird showed no response to any syllable of the BOS; the other

neuron responded at the second syllable, and the response was suppressed by deletion of the first or second syllable.
13. D. Margoliash, *J. Neurosci.* **3**, 1039 (1983); D. Margoliash, E. S. Fortune, *J. Neurosci.* **12**, 4309 (1992).
14. We gathered sufficient data from 14 neurons (from three birds) to permit quantitative comparisons between ongoing discharge and singing. Interspike interval histograms of the ongoing discharge of RA neurons during sleep are bimodal; the longer interval peak is related to nonbursting activity. Thus, bursts were defined as continuous sequences of interspike intervals falling outside of the normal (nonbursting) distribution of intervals.
15. Two tests of significance were devised. For each neuron, a distance was computed between each ongoing burst and the exemplar stretch of activity during singing. Each best match (lowest distance) was tested for significance by using a bootstrap procedure that assessed the probability of occurrence of the exact sequence of intervals observed in the burst. In the second test, for the one bird with the greatest number of recordings, we also compared each neuron's ongoing discharges during sleep with the premotor data from other neurons. For seven out of eight neurons, there were more matches with the neuron's own premotor data than with the premotor data from the other neurons. The same neuron failed to achieve significance in both tests.
16. The procedures for identifying bursts in ongoing activity, matching bursts to premotor activity, and assessing the significance of the matches are described in detail on *Science* Online (*24*).
17. M. Konishi, *Z. Tierpsychol.* **22**, 770 (1965).
18. C. E. Carr, W. Heiligenberg, G. J. Rose, *J. Neurosci.* **6**, 107 (1986); *J. Neurosci.* **6**, 1372 (1986); A. Moiseff, M. Konishi, *J. Neurosci.* **1**, 40 (1981); C. E. Carr, M. Konishi, *J. Neurosci.* **10**, 3227 (1990); G. Laurent, M. Wehr, H. Davidowitz, *J. Neurosci.* **16**, 3837 (1996); R. C. deCharms, M. M. Merzenich, *Nature* **381**, 610 (1996); A. K. Engel, P. R. Roelfsema, P. Fries, M. Brecht, W. Singer, *Cereb. Cortex* **7**, 571 (1997); Y. Prut *et al.*, *J. Neurophysiol.* **79**, 2857 (1998).
19. E. T. Vu, M. E. Mazurek, Y.-C. Kuo, *J. Neurosci.* **14**, 6924 (1994).
20. S. W. Bottjer, F. Johnson, *J. Neurobiol.* **33**, 602 (1997).
21. M. Luo, D. J. Perkel, *J. Neurosci.* **19**, 6700 (1999).
22. G. E. Hinton, P. Dayan, B. J. Frey, R. M. Neal, *Science* **268**, 1158 (1995).
23. G. Buzsáki, *Neuroscience* **31**, 551 (1989); M. A. Wilson, B. L. McNaughton, *Science* **265**, 676 (1994); W. E. Skaggs, B. L. McNaughton, *Science* **271**, 1870 (1996); Z. Nádasdy, H. Hirase, A. Czurkó, J. Csicsvari, G. Buzsáki, *J. Neurosci.* **19**, 9497 (1999).
24. Supplemental data are available at www.sciencemag.org/feature/data/1051099.shl.
25. We thank T. Q. Gentner, J.-M. Ramirez, P. S. Ulinski, and especially two anonymous reviewers for valuable comments on the manuscript. This work was supported by grants from the NIH (MH59831 and MH60276) to D.M. and (MH11615) to A.S.D.

6 April 2000; accepted 8 September 2000

Structure of Murine CTLA-4 and Its Role in Modulating T Cell Responsiveness

David A. Ostrov,[1,2] Wuxian Shi,[2] Jean-Claude D. Schwartz,[1] Steven C. Almo,[2]* Stanley G. Nathenson[1,3]*

The effective regulation of T cell responses is dependent on opposing signals transmitted through two related cell-surface receptors, CD28 and cytotoxic T lymphocyte–associated antigen 4 (CTLA-4). Dimerization of CTLA-4 is required for the formation of high-avidity complexes with B7 ligands and for transmission of signals that attenuate T cell activation. We determined the crystal structure of the extracellular portion of CTLA-4 to 2.0 angstrom resolution. CTLA-4 belongs to the immunoglobulin superfamily and displays a strand topology similar to Vα domains, with an unusual mode of dimerization that places the B7 binding sites distal to the dimerization interface. This organization allows each CTLA-4 dimer to bind two bivalent B7 molecules and suggests that a periodic arrangement of these components within the immunological synapse may contribute to the regulation of T cell responsiveness.

T cell–dependent immune processes require cell-surface interactions that mediate the initiation, modulation, and the ultimate course of the response. The specificity of T cell recognition is determined by the engagement of the T cell receptor (TCR) on T cells with cognate peptide–major histocompatibility complex (MHC) complexes presented by antigen-presenting cells (APCs) (*1*, *2*). Additional signals are required to sustain and enhance T cell activity, the most important of which is provided by the engagement of CD28 on T cells with its ligands B7-1 (CD80) and B7-2 (CD86) on APCs (*3*, *4*). In contrast, the interaction of B7 isoforms with CTLA-4, a CD28 homolog (31% identity), provides inhibitory signals required for down-regulation of the response (*5*).

Unlike CD28, which is expressed on resting T cells, CTLA-4 is not detected on the cell surface until 24 hours after activation, peaking at 36 to 48 hours after activation (*6*). In addition, CTLA-4 exhibits an affinity for the B7 isoforms that is 10 to 100 times that for CD28 (*7*). On the basis of these differences in expression patterns and affinities, it is likely that CTLA-4 directly competes with CD28 for binding B7 and also directs the assembly of inhibitory signaling complexes that lead to quiescence or anergy (*8*). Consistent with the inhibitory role of CTLA-4, mice deficient in CTLA-4 die as a consequence of unchecked polyclonal T cell expansion, which results in fatal lymphoproliferative disorders (*9*). Thus, the balance between the opposing signals elicited by CD28 and CTLA-4 is central to the regulation of T cell responsiveness and homeostasis (*10*).

Because of its dominant role in modulating T cell activity, CTLA-4 has received considerable attention as a therapeutic agent (*11*). The soluble CTLA-4–immunoglobulin (CTLA-4–Ig) fusion protein acts as an inhibitor of CD28-B7 costimulation and has specific inhibitory effects in animal models of autoimmunity, transplant rejection, asthma, and allergy (*3*, *12*). The efficacy of CTLA-4–Ig treatment of human disease has been demonstrated in clinical trials on patients with psoriasis vulgaris (*13*). This approach may well extend to a variety of T cell–mediated diseases including autoimmune diabetes, rheumatoid arthritis, systemic lupus erythematosus, and graft-versus-host disease (*13*). In contrast to strategies that interfere with the CD28-B7 association, reagents that interfere with the CTLA-4–B7 interaction intensify specific T cell responses. For example, blocking antibodies directed against CTLA-4 enhance rejection of preestablished tumors and protect against secondary challenge in animal models of prostate cancer and colon carcinoma (*14*).

The structure of the soluble extracellular domain of murine CTLA-4 (*15*) revealed two independent copies of the CTLA-4 dimer in the asymmetric unit of the crystal (Fig. 1, A and B, and Table 1) (*16*). The CTLA-4 monomer is a two-layer β-sandwich that exhibits the chain topology found in the immunoglobulin variable domains (Fig. 1A) (*17*). The front and back sheets, composed of strands A′GFCC′ and ABEDC″, respectively, are connected by two intersheet disulfide bonds. The disulfide bond between the B and F strands is a signature for the immunoglobulin fold; the disulfide bond joining strands C′ and D is unique to the CD28/CTLA-4 family (Fig. 1A) (*17*, *18*).

The nuclear magnetic resonance (NMR) structure of a monomeric form of human CTLA-4 (*18*) shows the same overall topology as the murine homolog, with a root mean square (rms) deviation of 2.4 Å between equivalent Cα atoms. The most significant

[1]Department of Microbiology and Immunology, [2]Department of Biochemistry, [3]Department of Cell Biology, Albert Einstein College of Medicine, Bronx, NY 10461. USA.

*To whom correspondence should be addressed. E-mail: almo@aecom.yu.edu or nathenso@aecom.yu.edu